12th IEA Heat Pump Conference 2017

Investigation on effects of piping on heating performance of multi-split variable refrigerant flow system

Ziai Li, Baolong Wang, Xianting Li, Wenxing Shi*

Dept. of Building Science, Tsinghua University, Beijing 100084, China

Abstract

To investigate the effects of piping on the heating performance of the multi-split VRF system under part-load conditions, a steady-state model of the multi-split VRF system in heating mode has been developed with its refrigerant pipeline model validated by an experiment. Then, the model was utilized to study the effects of horizontal pipe length and the height difference between the outdoor unit and the indoor units on the heating performance under part-load conditions. The results showed that under the control strategy of constant discharge pressure, the lengthening of horizontal pipe will reduce the COP apparently as the pipe length increased even under part-load conditions. It was indicated that the height difference in range from -50 m to 50 m had low effect on the COP but it would affect the available pressure drop of EEV. In application of the developed model, more work has been expected for a comprehensive evaluation on the multi-split VRF systems in buildings in the future.

© 2017 Stichting HPC 2017.
Selection and/or peer-review under responsibility of the organizers of the 12th IEA Heat Pump Conference 2017.

Keywords: Variable refrigerant flow system; piping; control strategy; simulation; heating performance

1. Introduction

The multi-split variable refrigerant flow (VRF) system has been widely applied in commercial buildings, hospitals and residential buildings in Asian and European countries for space cooling and heating since its beginning in 1980s, due to its features of space saving, efficient part-load performance and excellent individual independent control for separate zones. Generally, the multi-split VRF system is composed of one outdoor unit and multiple indoor units connected by refrigerant pipelines, wherein the refrigerant flow rate through each indoor unit can be adjusted by the respective electronic expansion valve (EEV). Up to now, several types of multi-split VRF systems, e. g., heat recovery type and water-cooled type, have been introduced, among which the air-cooled heat pump type is dominating. Usually, the outdoor unit is located on the top or ground out of the building, therefore the refrigerant pipeline length and height difference between the outdoor unit and indoor units are inevitable. To extend the application of multi-split VRF systems in high-rise and large-sized buildings,

the refrigerant pipeline of the system has been enlarged a lot. The allowable outdoor-to-indoor pipeline length can be up to 149m and the allowable height difference between the outdoor unit and indoor units can be up to 46m [1].

However, an issue of performance degradation caused by the enlargement of piping in the application of multi-split VRF systems arises. In the summer of 2005, a field test on the multi-split VRF systems whose outdoor units were located on the top of the office building in Beijing showed that, in the part-load ratio range of 50-78%, the average cooling COP of multi-split VRF systems on 1st floor, 5th floor and 7th floor is 2.92, 3.11 and 3.32, respectively [2], To qualitatively analyze, 1) in the cooling mode, as the suction gas pipe length increases, the suction pressure decreases while the evaporating temperature and the suction superheated degree increase due to the frictional pressure drop, which will result in the reduction of the compressor volumetric efficiency, the cooling capacity and the cooling COP; 2) in the heating mode, as the discharge gas pipe length increases, the condensing temperature will decrease which results in the heating capacity degradation; 3) the height difference between the outdoor unit and indoor units causes the gravitational pressure drop of rise in the liquid pipe, therefore leading to the insufficiency or surplus of the available pressure drop of the EEVs in the indoor units.

Great attentions have been attracted on this issue. A study on the heat pump type multi-split VRF system with R22 under the rated conditions concluded that, when the pipe length exceeds 60 m and 95 m, the total cooling/heating COP of the system will be lower than that of the air-cooled water chiller/heater combined with fan coil unit system [3]. Most of the VRF manufacturers offer users with the curves of the rated cooling and heating capacity degradation ratio related to the pipeline length and height difference, which are necessary for the design of multi-split VRF systems in buildings [4-7]. Additionally, there are some investigations on the influence of pipeline length and height difference on the cooling performance of the multi-split VRF system under various conditions, either by experiment or by simulation [8-11]. However, few studies are available concerning the effects of piping on part-load heating performance with consideration of the control strategy.

Therefore, with the purpose of learning the effects of piping on part-load heating performance of the multi-split VRF system, a steady-state model of a multi-split VRF system in heating mode was developed in this study. Then, the model was applied to predict the heating performance of a designed multi-split VRF system under different pipeline length and height difference. Finally, the results were discussed for the evaluation of piping effect on the heating energy performance of the multi-split VRF system.

Nomenclature

COP	coefficient of performance, W/W
D_i	internal diameter, m
e	relative error or absolute error
e'	acceptable relative error or absolute error
f	friction factor
f_{L0}	friction factor of liquid
g	gravitational acceleration, m/s^2
h	enthalpy, J/kg
j	serial number of each indoor unit
J	mass flux, kg/(m^2 s)
l	length, m
m	mass flow rate, kg/s
N	number of indoor units
P	pressure, Pa
Qc	heating capacity, W
Re	Reynolds number

T	temperature, °C
W	power input, W
x	refrigerant vapor quality
x_{eev}	the opening ratio of EEV

Greek symbols

α	void fraction of gas-liquid two phase refrigerant
ΔTsh	superheated degree , °C
ε	absolute roughness of pipe wall, m
η_s	isentropic efficiency
η_v	volumetric efficiency
ρ	density, kg/m^3
ϕ_{L0}^2	two-phase flow resistance correction coefficient

Subscripts

c	condenser
cp	compressor
dis	discharge
e	evaporator
eev	electronic expansion valve
f	friction
G	gas
h	enthalpy
i	inlet
L	liquid
m	mass flow rate
mass	mass charge
MGP	main gas pipe
MLP	main liquid pipe
o	outlet
od	outdoor
p	pressure
s	isentropic process
set	preset value
SGP	secondary gas pipe
SLP	secondary liquid pipe
suc	suction

2. Model development

As shown in Fig. 1, a typical air-cooled heat pump multi-split VRF system operates in heating mode with the indoor heat exchangers working as condensers while the outdoor heat exchanger working as a evaporator. The discharged high-pressure gas refrigerant out of the compressor flows through the gas pipes into the indoor heat exchangers and then supplies heat in a condensation process. The subcooled refrigerant out of the indoor heat exchangers became a gas-and-liquid phase through the indoor EEVs and then flows through the liquid pipes to the outdoor unit. The model developed is based on the model for cooling mode reported in the previous study by the authors [10], which was modified to apply to the heating mode in this study.

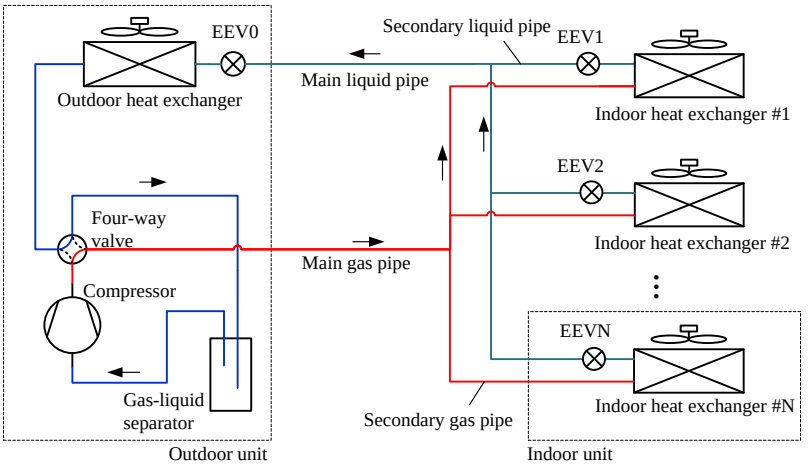


Fig. 1. A typical air-cooled heat pump multi-split VRF system operating in heating mode

2.1. Sub-models

The sub-models of compressor, fin-and-tube heat exchanger, EEV, thermodynamic properties of R410A and moist air used in this study can be found in the reference [10], therefore not elaborated here. Herein, it was assumed that no frosting occurred in the outdoor heat exchanger and the gas-liquid separator was neglected, which is acceptable for a steady-state modeling.

As for the refrigerant pipeline concerned, the heat exchange along was calculated using the nullity fin tube heat exchanger model which was a simplified form of the fin-and-tube heat exchanger model [12]. The pressure drop along the refrigerant pipeline, which is the sum of friction pressure drop, potential pressure drop and acceleration pressure drop, was taken seriously. The refrigerant pipe is wrapped by insulation and there is no change in pipe diameter, and therefore the acceleration pressure drop can be neglected. The friction pressure drop was calculated by the distributed-parameter method using the following model reported by Churchill [13] and Zhou [14]:

Single-phase:
$$-\left(\frac{dP_{\mathrm{f}}}{dl}\right)=\frac{f}{2D_{\mathrm{i}}}\cdot\frac{J^{2}}{\rho} \tag{1}$$

$$f=8\left[\left(8/Re\right)^{12}+K^{-1.5}\right]^{1/12} \tag{2}$$

$$K=\left(\frac{37530}{Re}\right)^{16}-\left[2.457\ \ln\left(\left(\frac{7}{Re}\right)^{0.9}+0.27\frac{\varepsilon}{D_{\mathrm{i}}}\right)\right]^{16} \tag{3}$$

Two-phase: $$-\left(\frac{dP_{\mathrm{f}}}{dl}\right)=\frac{f_{\mathrm{L0}}}{2D_{\mathrm{i}}}\cdot\frac{J^{2}}{\rho_{\mathrm{L}}}\cdot\phi_{\mathrm{L0}}^{2} \tag{4}$$

$$f_{\mathrm{L0}}=8c\cdot Re^{-k} \tag{5}$$

$$\phi_{\mathrm{L0}}^{2}=1+(Y^{2}-1)[bx^{(2-q)/2}(1-x)^{(2-q)/2}+x^{(2-q)}] \tag{6}$$

where the values of the empirical coefficients, *c* and *k*, were 0.046 and 0.2, respectively. The value of the Blasius resistance index, *q*, was 0.25 and the values of the Chisholm factor and empirical coefficient, *Y* and *b*, were obtained from the list provided by Zhou [14].

The potential pressure drop was calculated using the basic equations:

$$-\left(\frac{dP_{\mathrm{z}}}{dz}\right)=\rho_{\mathrm{L}}\cdot g\cdot\{1-\alpha(1-\frac{\rho_{\mathrm{G}}}{\rho_{\mathrm{L}}})\} \tag{7}$$

Based on the above sub-models, as well as the energy conservation, momentum conservation and mass conservation equations, the system model was developed and was solved by the procedure as shown in Fig. 2.

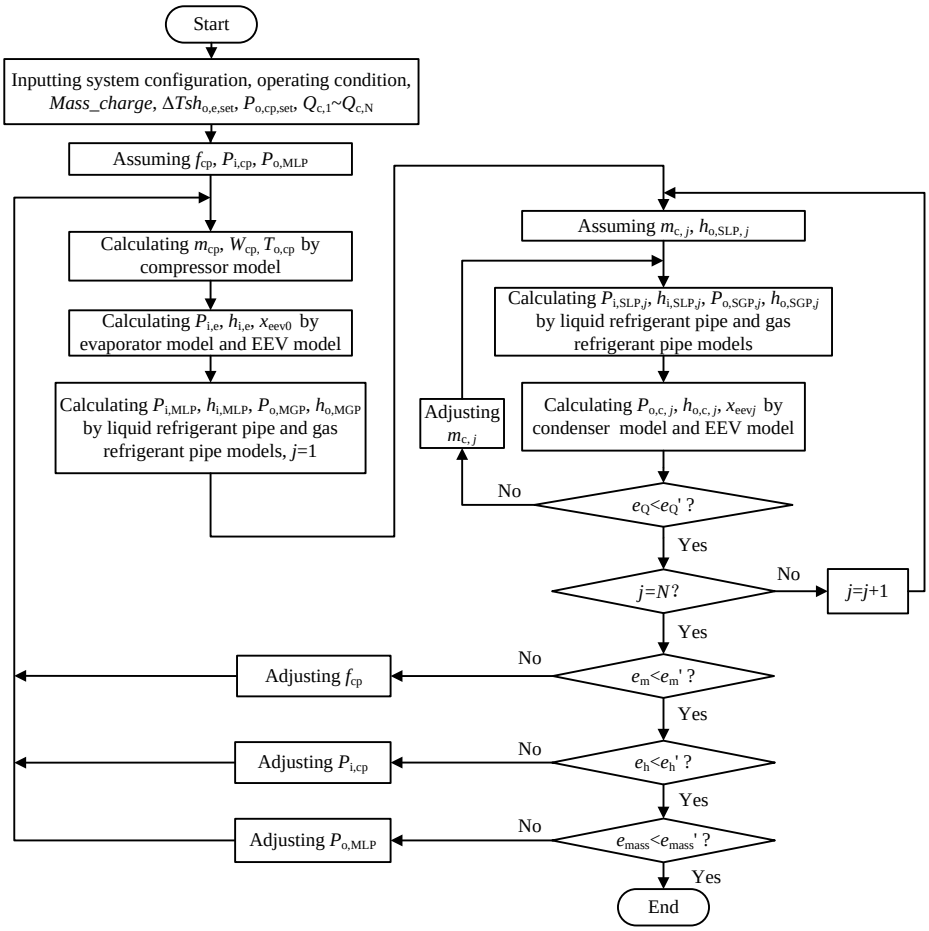


Fig. 2. Solving procedure for the developed multi-split VRF system model in heating mode

2.2. Validation of refrigerant pipeline model

Since the study concentrates on the refrigerant pipeline, an experiment on a data center room air-conditioner equipped with long connecting pipe was conducted to validate the refrigerant pipeline model. As shown in Fig.3, the experimental system consists of one indoor unit, which includes a 5 HP variable-speed compressor and the evaporator, and one outdoor unit which contains a condenser. The indoor unit was located 30 m higher than the outdoor unit, connected by a 100-meter-long liquid pipe (the nominal diameter is 15.88 mm) and a 100-meter-long gas pipe (the nominal diameter is 19.05 mm) with the latter unit. The connecting pipes were wrapped with 18 mm insulation material. A number of temperature sensors and pressure sensors were separately positioned at the compressor suction tube, the compressor discharge tube, the inlets and outlets of liquid pipe and gas pipe for measurement, as shown in Fig. 3. Though there was no mass flow meter in this simple test bench, the refrigerant mass flow rate could be calculated based on the measured refrigerant states at the suction and discharge tubes of the compressor by employing the compressor efficiency model [15] mentioned in Section 2.1. The volumetric efficiency and isentropic efficiency formulas demanded in the compressor efficiency model were regressed according to the compressor performance curves provided by the

manufacture. The calculated mass flow rate was assumed to represent the real value of the factory-fresh compressor.

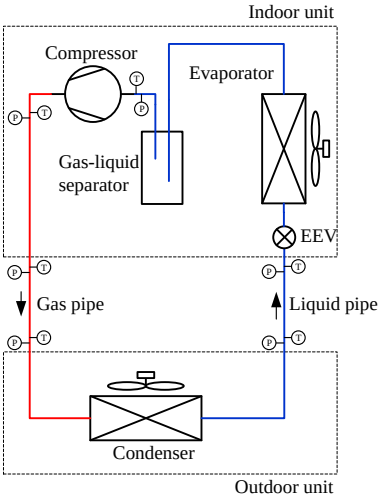


Fig. 3. Schematic of experimental data center room air-conditioner for validation of pipeline model

As shown in Table 1, ten validation cases with various compressor frequencies and various ambient temperatures were carried out in the experiment. Then, the refrigerant mass flow rates and pressure drop along the gas pipe and the liquid pipe in the ten cases were calculated as summarized in the table. In comparison with the measured values, the deviation of the calculated pressure drops in the gas pipe and the liquid pipe using the developed pipeline model were within ±27.0 %, which is acceptable on an engineering level in this study.

Table 1. Results from measurement and simulation in ten validation cases

Ambient temperature (ºC)		45			35			25		
Compressor frequency (Hz)		84	70	50	84	70	50	84	70	50
Measurement	Suction temperature (ºC)	34.5	36.4	40.3	32.6	34.8	38.4	27.1	30.8	35.2
	Suction pressure (MPa)	1.136	1.221	1.174	1.102	1.181	1.182	1.096	1.181	1.322
	Discharge pressure (MPa)	3.612	3.478	3.205	2.953	2.818	2.567	2.631	2.547	2.418
	Gas pipe pressure drop (MPa)	0.160	0.120	0.037	0.217	0.169	0.075	0.286	0.241	0.125
	Liquid pipe pressure drop (MPa)	0.304	0.293	0.267	0.311	0.301	0.275	0.318	0.306	0.288
Simulation	Refrigerant mass flow rate (kg/h)	446.2	399.2	259.1	432.6	380.1	256.2	443.3	387.9	292.4
	Gas pipe pressure drop (MPa)	0.155	0.121	0.043	0.191	0.148	0.074	0.227	0.173	0.092
	Liquid pipe pressure	0.295	0.297	0.290	0.334	0.333	0.315	0.360	0.347	0.330

	drop (MPa)								
Deviation of simulation	Gas pipe pressure drop	-3.1%	0.8%	16.2%	-12.0%	-21.4%	-1.3%	-20.6%	-19.2%	-26.4%
	Liquid pipe pressure drop	-3.0%	1.4%	8.6%	7.4%	10.6%	14.6%	13.2%	13.4%	14.6%

3. Cases studied

Utilizing the developed model, the heating performance of a designed multi-split VRF system with various pipeline length and height difference between the outdoor unit and the indoor units was predicted. The system consists of one outdoor unit and four identical indoor units. The designed compressor displacement was 85 cm^3/rev and the adopted volumetric efficiency (η_v) and isentropic efficiency (η_s) expressions in relation to compressor frequency (f_{cp}), suction saturation temperature ($T_{s,suc}$) and discharge saturation temperature ($T_{s,dis}$) were listed in Table 2.

Table 2. Volumetric efficiency and isentropic efficiency expressions for the designed compressor

Output/Input	Curve 1	Curve 2	Output/Input	Curve 1	Curve 2	Output/Input	Curve 1	Curve 2
U	η_v	η_s	a_5	-3.596E-6	-4.610E-4	a_{14}	-5.104E-7	-5.194E-7
X	f_{cp}	f_{cp}	a_6	-1.275E-4	1.012E-4	X min	20	20
Y	$T_{s,suc}$	$T_{s,suc}$	a_7	-1.172E-4	-1.890E-4	X max	120	120
Z	$T_{s,dis}$	$T_{s,dis}$	a_8	1.473E-4	5.499E-4	Y min	-10	-10
a_0	1.090	2.205	a_9	2.284E-4	2.082E-4	Y max	20	20
a_1	-4.838E-3	-1.442E-2	a_{10}	9.748E-7	1.202E-6	Z min	35	35
a_2	-2.215E-3	3.454E-3	a_{11}	-1.122E-6	-1.524E-6	Z max	60	60
a_3	9.235E-4	-3.599E-2	a_{12}	6.558E-7	1.967E-6			
a_4	3.019E-5	2.677E-5	a_{13}	5.759E-7	-2.403E-6			

Note: Curve 1- Volumetric efficiency curve; Curve 2- Isentropic efficiency curve;
$U=a_0+a_1X+a_2Y+a_3Z+a_4X^2+a_5Y^2+a_6Z^2+a_7XY+a_8XZ+a_9YZ+a_{10}X^2Y+a_{11}X^2Z+a_{12}XY^2+a_{13}XZ^2+a_{14}XYZ$ (for Curve 1 and Curve 2)

With a rated compressor frequency of 60 Hz, the specifications of the heat exchanger were determined to output a rated cooling capacity of 28 kW under the standard cooling condition, where the lengths of main/secondary gas pipe and the main/secondary liquid pipe were 5.0 m and the outdoor/indoor air dry-bulb temperature was 35ºC/27ºC. The structural parameter values of the designed heat exchangers were listed in Table 3. As seen in Fig.1, the nominal diameters of EEV0 and EEVN were 6.0 mm and 2.4 mm, respectively. The nominal diameters of the main gas pipe, the main liquid pipe, the secondary gas pipe and the secondary liquid pipe were 25.4 mm, 12.7 mm, 15.88 mm and 9.53 mm, respectively. Those pipes were wrapped with 18 mm insulation material. The refrigerant mass charge, which was the circulating refrigerant mass in fact in this study, was 3.0 kg and was added 0.11 kg/m when the main liquid pipe was extended.

Table 3. Structural parameters of the designed heat exchangers

	Quantity	Structural parameter											
		k	n_t	r	l	s_1	s_2	D_o	D_i	th	s_3	V_a	Fin type
Outdoor heat exchanger	1	12	60	4	950	22	25.4	9.52	8.8	0.105	1.8	11000	Plain
Indoor heat exchanger	4	2	6	3	465	22	25.4	9.52	8.8	0.105	1.8	980	Wavy

In the study case, the control strategy of constant discharge pressure was utilized for analysis. The corresponding setpoint of discharge saturation temperature was 54ºC, which was controlled by modulating the compressor frequency. The outlet refrigerant of the outdoor heat exchanger was superheated by 5ºC by regulating EEV0, while the indoor EEV0~EEVN were modulated to meet the heating demand of each air-conditioned room. For simulation analysis, the length of main gas pipe and main liquid pipe varied from 5 m to 165 m, with the secondary gas pipe and the secondary liquid pipe in constant length of 5 m. The height difference between the outdoor unit and the indoor units varied from -50 m to 50 m (positive when the outdoor unit was located higher), while the four indoor units were kept on the same horizontal level. The outdoor/indoor air dry-bulb temperature was 7 ºC/20 ºC and the outdoor relative humidity was 50% in all cases.

4. Results and discussion

4.1. Effect of pipeline length

The performance of the designed multi-split VRF system with different lengths of main pipes under various heating demand from 18.8 kW to 26kW was predicted, with no height difference between the outdoor unit and indoor units. As seen in Fig. 4, as the main gas pipe and main liquid pipe length increased from 5 m to 165m, under the constant discharge pressure control strategy, the system was forced to run at a higher compressor speed to promote the mass flow rate to output the same heating amount due to the drop of condensing temperature, which can be reflected by the inlet pressure of condenser. The inlet pressure of condensers reduced with 0.068 MPa, which indicated about 1ºC of condensing temperature drop, as the main pipe was lengthened from 5 m to 165 m when the heating capacity *Qc* was 26 kW. As seen from Fig. 5, the COP, which was defined as the heating capacity divided by the compressor power input in the simulation cases, declined greatly as the pipe length increased from 5 m to 165m with a similar descending rate at *Qc* of 18.8 kW to 26 kW, e.g., the COP decreased from 3.28 to 3.11 at *Qc*=26 kW. Therefore, under the control strategy of constant discharge pressure, the increasing pipe length had a negative effect on the heating energy performance, which should be taken into account in the real-performance evaluation of the multi-split VRF system.

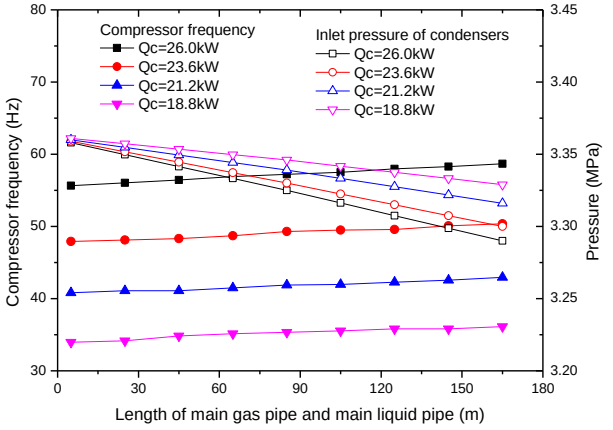


Fig. 4. Compressor frequency and inlet pressure of condensers with various main pipe lengths

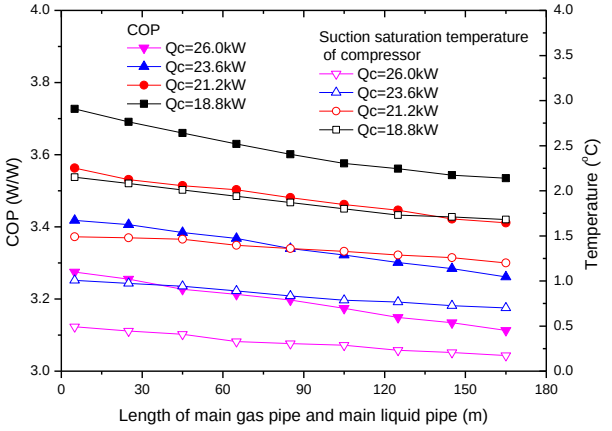


Fig. 5. COP and suction saturation temperature of compressor with various main pipe lengths

4.2. Effect of height difference

For the designed multi-split VRF system with different height difference between the outdoor unit and indoor units, its predicted heating performance under various heating demand from 18.8 kW to 26kW was shown in Fig. 6 and Fig. 7. As the height difference changed from -50 m to 50 m, the compressor and COP showed little change (in fact there was a tiny decrease of COP caused by length increasing) while the outlet subcooling degree of condensers increased slightly. Comparatively, as the height difference changed from -50 m to 50 m, the available pressure difference for EEV0 decreased markedly, e.g., the available pressure difference decreased from 2.25 MPa to 1.55 MPa at *Qc*=26 kW. The insufficiency or surplus of available pressure difference of EEV would greatly influence its adjustability and system stability. Therefore, the height difference should be restricted in the design of multi-split VRF systems in buildings.

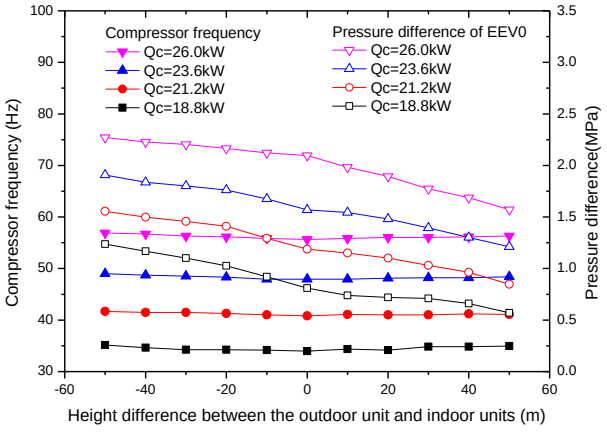


Fig. 6. Compressor frequency and pressure difference of EEV0 with various height differences

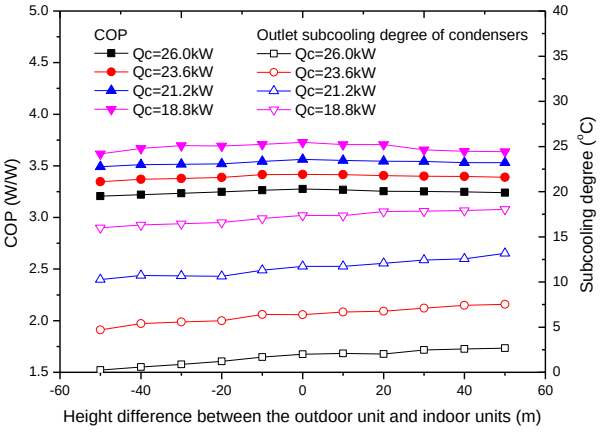


Fig. 7. COP and outlet subcooling degree of condensers with various height differences

5. Conclusion

The effects of piping on heating performance of the multi-split VRF system under part-load conditions have not yet been investigated despite the rated capacity degradation curves of products provided by ~~manufactories~~manufacturers. This study has developed a steady-state model of the multi-split VRF system in heating mode, in which the refrigerant pipeline model was validated by an experiment. Following the design of a multi-split VRF system, the impacts of the lengths of the gas pipe and the liquid pipe and the height difference between the outdoor unit and the indoor units on the heating performance under part-load conditions were predicted utilizing the developed model under the constant discharge pressure control strategy. The results showed that the lengthening of horizontal pipe will reduce the COP apparently as the pipe length increased even under part-load conditions. It was indicated that the height difference in range from -50 m to 50 m had

low effect on the COP but it would affect the available pressure drop of EEVs, which should be therefore restricted in the design of the multi-split VRF systems in buildings. The efforts to learn the performance of the multi-split VRF systems affected by piping under part-load conditions is of great value for saving energy and long-period energy evaluation in its application. In future work, the developed model will be further applied to study the effect of piping under more operation conditions and different control strategies, aiming at a comprehensive evaluation on the application of multi-split VRF systems in buildings.

Acknowledgements

The study has been supported by the China National Key R&D Program "Solutions to heating and cooling of buildings in the Yangtze river region" (Grant No. 2016YFC0700304) and the Innovative Research Groups of the National Natural Science Foundation of China (grant number 51521005).

References

[1] R. Afify, Designing VRF systems, 2008. ASHRAE Journal, 50: 52-55.
[2] Department of Building Science, Tsinghua University, 2005. Reports on public building energy saving diagnosis in the summer of 2005. Beijing, China. (in Chinese)
[3] W. Shi, S. Shao, Q. Yan, 2007. Effctive region of multi-connected air-conditioner (heat pump) system. Journal of Refrigeration, 28(2): 8-12. (in Chinese)
[4] Daikin (China) investment Co., Ltd, 2008. VRV system design manual.
[5] Liu X, Hong T, 2010. Comparison of energy efficiency between variable refrigerant flow systems and ground source heat pump systems. Energy and Buildings, 42(5): 584-589.
[6] Raustad R, 2012. Creating performance curves for variable refrigerant flow heat pumps in EnergyPlus. Report: FSEC-CR-1910-12, Florida Solar Energy Center.
[7] Samsung (China) investment Co., Ltd, Samsung digital central air-conditioning system technical information.[8] Z. Guo, 2007. An experimental study of the influence of refrigeration pipe length on the performance of multi-connected air-conditioning systems. Master of Engineering Thesis, Qingdao Technological University, Qingdao, China. (in Chinese)
[9] Pan Yan, Xu Xiangguo, Xia Liang, Deng Shiming, 2012. A modeling study on the effects of refrigerant pipeline length on the operational performance of a dual-evaporator air conditioning system. Applied Thermal Engineering, 39:15-25.
[10] Li Z, Wang B, Li X, Shi W, 2016. Simulation on effects of subcooler on cooling performance of multi-split variable refrigerant flow systems with different lengths of refrigerant pipeline. Energy and Buildings, 126: 301-309.
[11] Hong T, Sun K, Zhang R, Hinokuma R, Kasahara S, Yura Y, 2016. Development and validation of a new variable refrigerant flow system model in EnergyPlus. Energy and Buildings, 117: 399-411.
[12] S. Shao, X. Li, W. Shi, Q. Yan, 2003. A universal simulation model of air-cooled condenser consisting of plate-fin-tube, in: Proceedings of 2003 ASME Summer Heat Transfer Conference, Las Vegas, Nevada, USA, July 21–23, pp. 729-734, Paper No. HT2003-47405.
[13] S. W. Churchill, 1977. Friction-factor equation spans all fluid-flow regimes. Chemical Engineering 84: 91-92.
[14] Q. Zhou, 1990. Two-phase flow and heat transfer. Water Resources and Electric Power Press, Beijing (in Chinese).
[15] R. Koury, L. Machado, K. Ismail, 2001. Numerical simulation of a variable speed refrigeration system, International Journal of Refrigeration 24: 192-200.